Antenna Designs Showing Riemann Zeros

Brian Scannell August 2021
brian.scannell@ntlworld.com

Abstract

The nulls in antenna radiation patterns show the non-trivial Riemann zeta zeros. Here we simulate antenna designs that show the zeros

Background

van der Pol (VDP) [1] used an electromechanical method to visualise the Riemann zeros. He showed the Fourier transform of the function $f(u) = e^{\frac{1}{2}u} - e^{-\frac{1}{2}u}\lfloor e^u \rfloor$, where $\lfloor e^u \rfloor$ is the floor function, is real and is related to the Riemann zeta function on the critical line $-\frac{\zeta(1/2+it)}{1/2+it}$. The VDP function *f(u)* has a saw-tooth form shown in Figure 1.

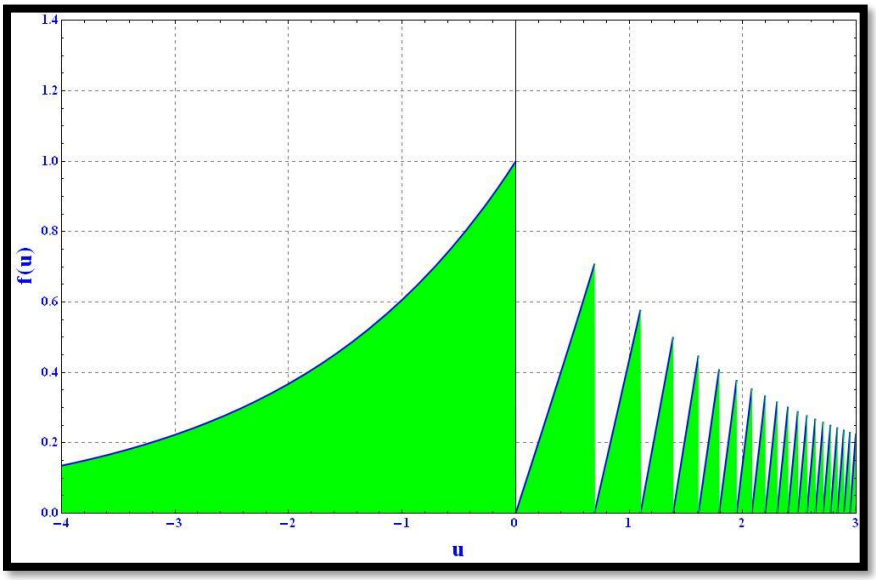

Figure 1 The van der Pol function f(u)

Berry [2] noted that since an antenna far-field radiation pattern is the Fourier transform of its aperture field it could be feasible to observe the zeta zeros in the nulls of an antenna pattern with an aperture field of the form *f(u)*.

The sampling effect in viewing the zeros

The radiation pattern function $g(t)$ is the Fourier transform of the aperture function -*f(u)* and gives the zeta function on the critical line, with t the height on the critical line,

$$g(t) = \frac{\zeta(1/2+it)}{1/2+it} = \int_{-\infty}^{\infty} \left[e^{-\frac{1}{2}u} \lfloor e^u \rfloor - e^{\frac{1}{2}u} \right] . e^{-itu} du$$

An antenna has a finite aperture and therefore the Fourier transform will be truncated. This affects the visibility of the pattern nulls and therefore the zeta zeros.

Figure 2 compares the untruncated *g(t)* to the numerical computation of the truncated discrete Fourier transform $G(t) = \int_{-u\max}^{u\max} \left[e^{-\frac{1}{2}u} \lfloor e^{u} \rfloor - e^{\frac{1}{2}u} \right] . e^{-itu} du$ for umax=3, 5, 10 and 15 with sampling interval *du* equal to 0.01. The resolution dt is $2\pi / u_{span}$ where $u_{span} = 2u_{\max}$ giving dt as 1.047, 0.628, 0.318 and 0.209.

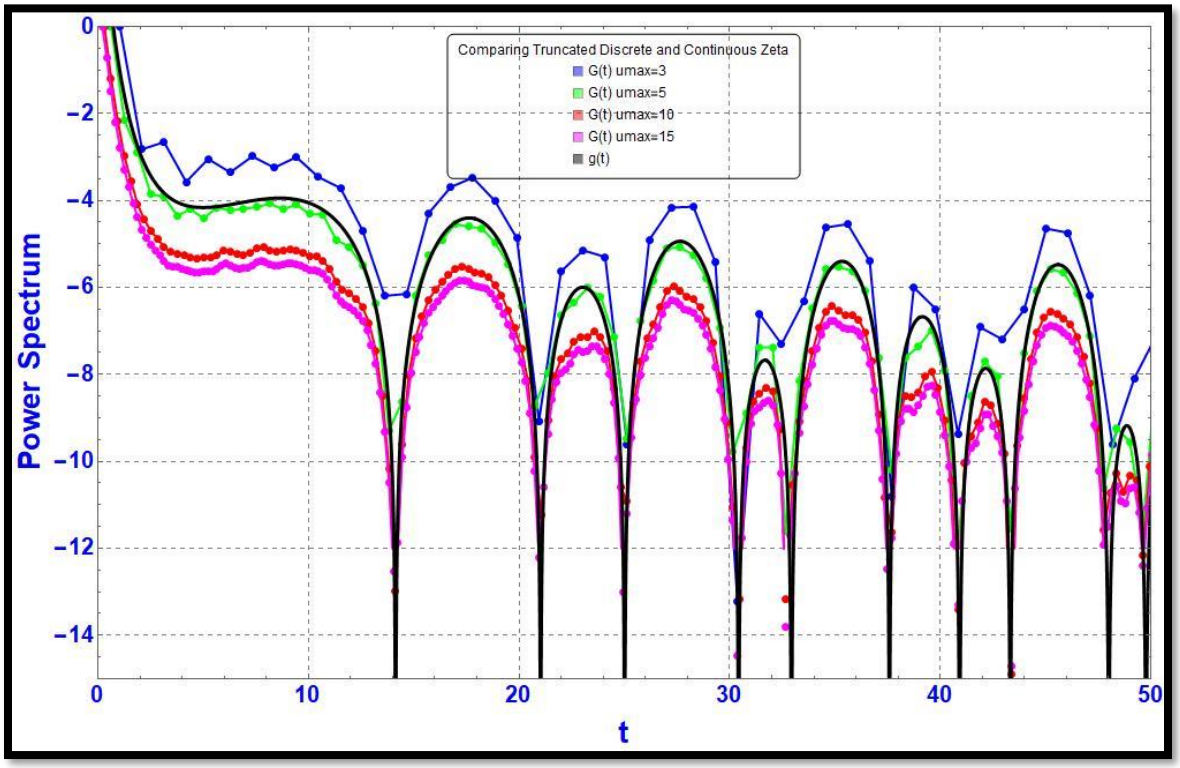

Figure 2 Comparing g(t) and G(t) for umax=3, 5, 10 and 15

In order to keep the antenna small for manufacturing and test purposes umax is chosen as 3 accepting the reduced visibility of the nulls.

Relationship to antenna design

Let an antenna aperture in the x direction have a discrete number of voltage sources separated by *dx* each with an electric field amplitude given by the VDP function *f(u)*. Antenna theory gives the far field radiation pattern as the Fourier transform of the aperture electric field. The radiation pattern is plotted as gain relative to an isotropic source (dBi) versus angle in degrees. Berry [2] shows the angle of the pattern nulls θ_n are related to the heights of the zeros t_n given here by

$\sin\theta_n = \pm \frac{t_n du}{kdx}$ with kdx / du being the largest height visible.

Practical antenna measurement frequency range

Microwave frequency antennas are designed and tested generally in the range 0.5 to 40GHz. Here we use 40GHz in order to reduce the size of the antenna for practical test purposes.

brian.scannell@ntlworld.com

Theoretical dipole antenna design

The first antenna design is an array of 40GHz dipoles shown in Figure 3. There are 601 dipoles separated in x by 0.8mm. The red triangles represent the feed points which have been given a voltage following the VDP function with umax=3 and du=0.01.

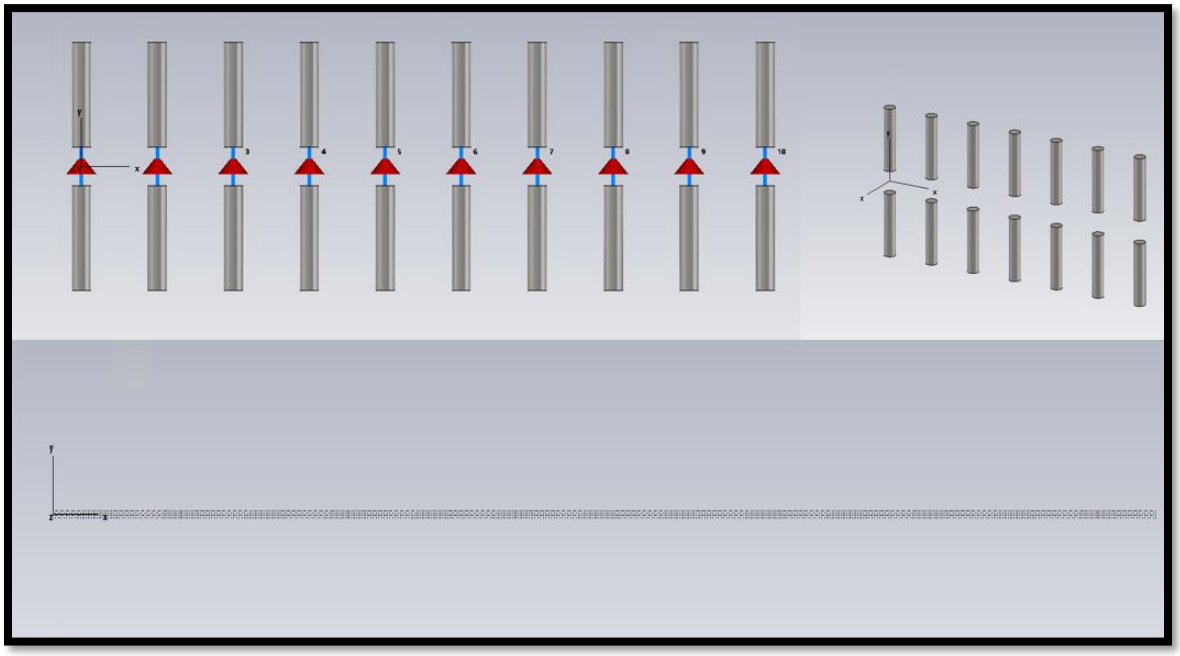

Figure 3 An array of 601 40GHz dipoles.

The radiation patterns are computed using commercial antenna design software CST (Computer Simulation Technology). This is a full-wave simulation using a numerical evaluation of Maxwell's equation with accuracy only limited by the discretization of the model.

Figure 4 shows views of the computed 3D radiation patterns.

brian.scannell@ntlworld.com

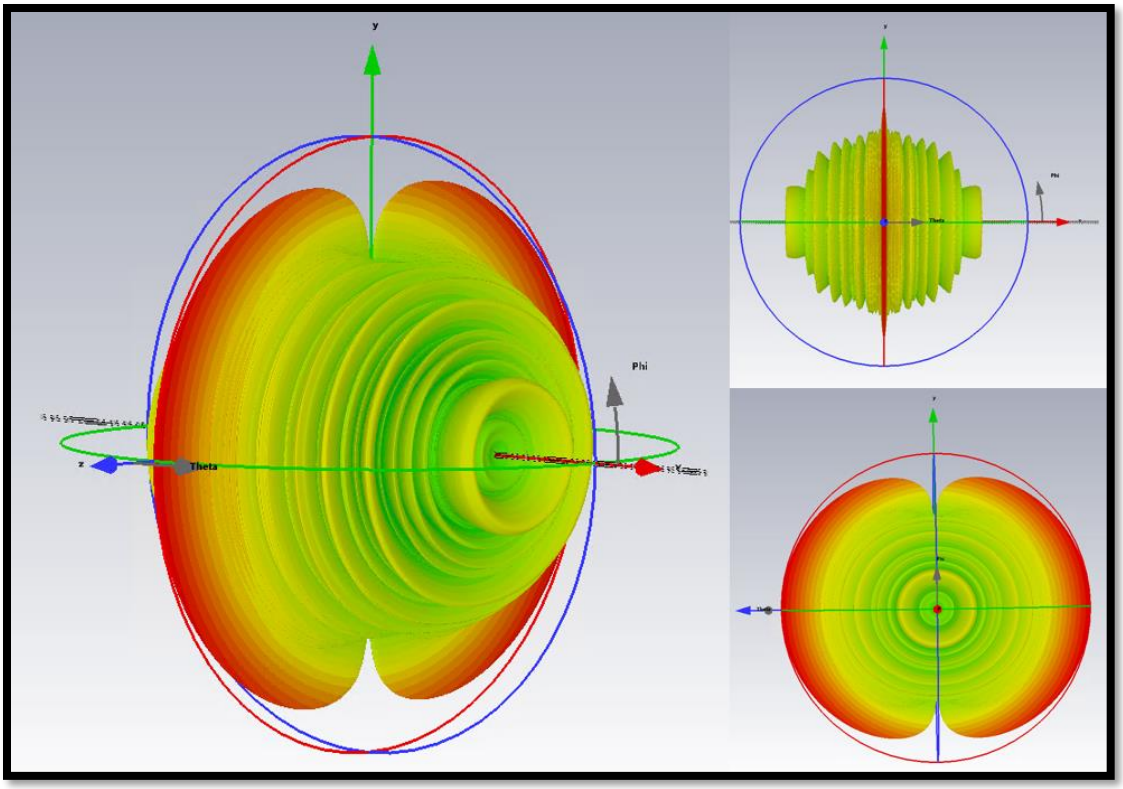

Figure 4 Computed 3D radiation patterns of the 40GHz dipole array

The zeros are visible in Figure 5 which is a Cartesian cut showing antenna directivity dBi versus $\theta°$ for $\phi = 0°$. The visible limit on the height of the zeros is $k\,dx/\partial u$ which is about 67.

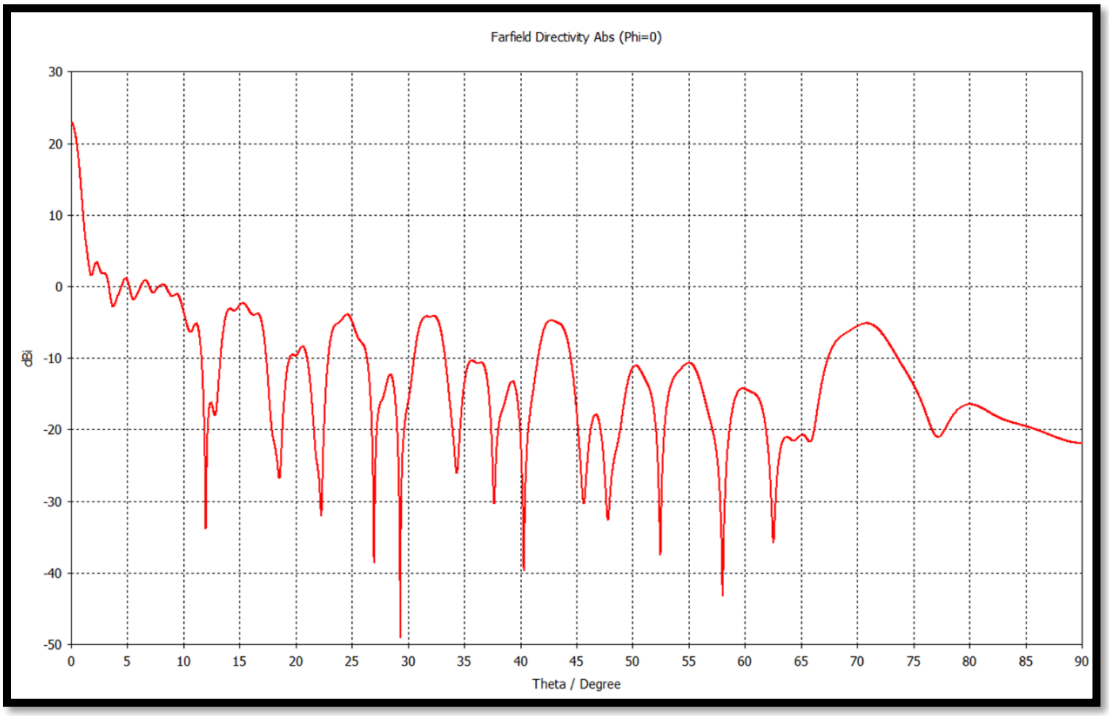

Figure 5 Dipole radiation pattern with nulls representing the zeta zeros

brian.scannell@ntlworld.com

Conversion from angles to number are given in Table 1 showing the radiation patterns exhibit the zeros with errors generally less than 1%. The results in blue are poorly formed nulls.

Zero Number	Sidelobe Null Angle deg	Observed Zero	Zeta Zero	Error %
1	12.00	13.95	14.13	-1.3
2	18.56	21.36	21.02	1.6
3	22.25	25.40	25.01	1.6
4	26.97	30.43	30.42	0.0
5	29.29	32.82	32.94	-0.4
6	34.34	37.85	37.59	0.7
7	37.67	41.00	40.92	0.2
8	40.32	43.41	43.33	0.2
9	45.64	47.96	48.01	-0.1
10	47.82	49.71	49.77	-0.1
11	52.49	53.22	52.97	0.5
12	58.03	56.91	56.45	0.8
13	62.55	59.53	59.35	0.3
14	64.42	60.51	60.83	-0.5
15	65.79	61.19	65.11	-6.0
16	77.09	65.39	67.08	-2.5

Table 1 Zeros shown by the radiation pattern of an array of dipoles. Blue entries are not clear nulls

However, this is not a practical antenna design since there is no method to produce the dipole voltages.

A more practical slot array antenna design

Slots in a ground plane can be used to diffract a plane electromagnetic wave. The plane wave excites each slot with the VDP voltage.

Figure 6 shows an array of 601 slots with 0.8mm spacing in the longer y direction. The slot width is 5mm in the x direction with the length in the y direction designed empirically to yield an electric field strength within the slot that follows the VDP form with umax=3 and du=0.01. The antenna dimensions are 500mm in the y direction by 50mm in the x direction. The method of fabrication would use printed circuit board (PCB) technology of photo-etching commercially available 35um thick copper-clad dielectric laminates. The manufacturing process limits the minimum slot width to around 30um. The maximum slot length is 750um to prevent overlapping slots.

Again, the visible limit on the height of the zeros is $k\,dy/\partial u$ which is about 67.

brian.scannell@ntlworld.com

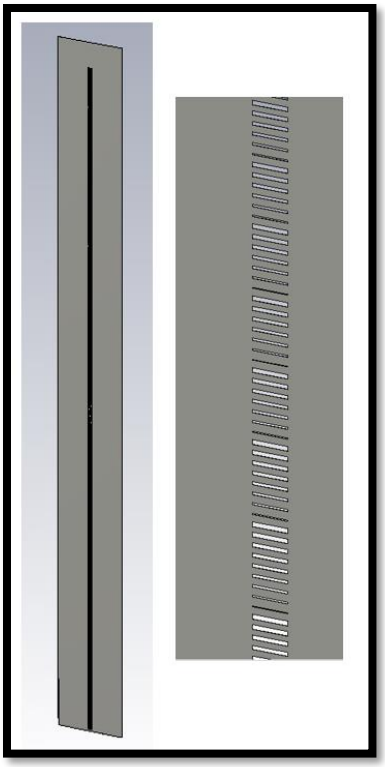

Figure 6 A slot array in a thin 35 micron metal ground plane with the 5mm slot width in the x direction

Figure 7 shows the computed electric field amplitude as vector cones in a plane 0.15mm just above the slots. The longer slots have higher electric fields.

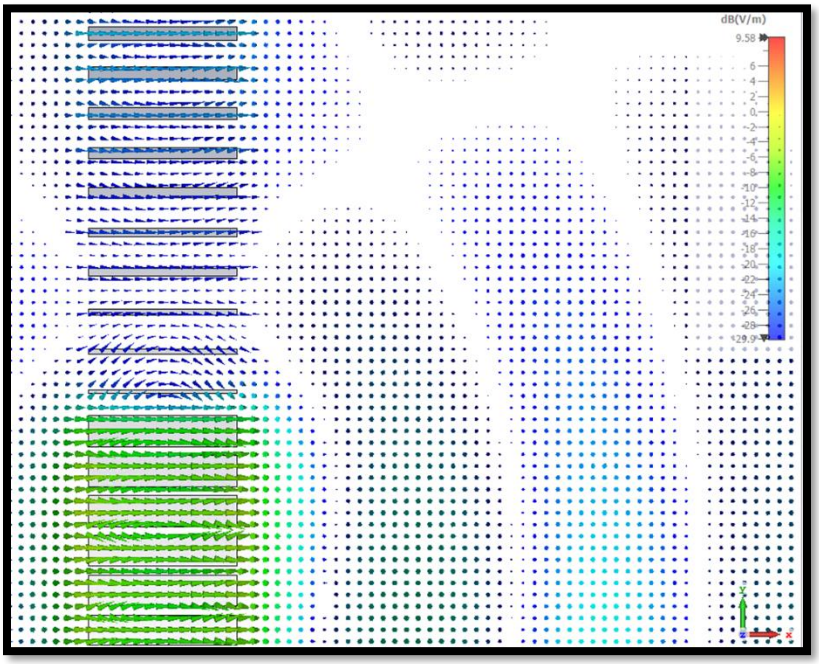

Figure 7 The electric field just above the slots (0.15mm)

brian.scannell@ntlworld.com

Figure 8 shows the electric field amplitude at the center of the slots in the y direction which approximates the VDP function. This amplitude decreases further away from the slots (z=1mm).

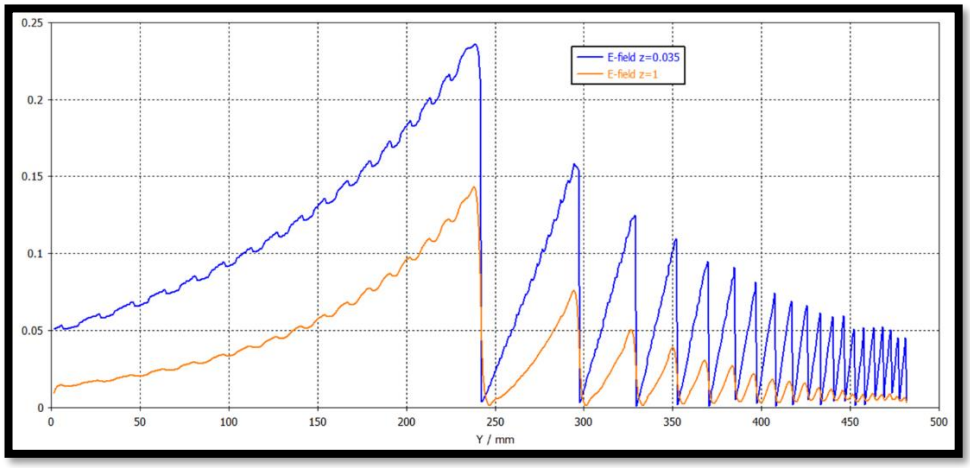

Figure 8 The y variation of electric field amplitude at the slot centers plotted at two heights (mm) above the slot

The radiation pattern of this slot array is shown in Figure 9. This is the diffraction pattern of an incident plane electromagnetic wave travelling in the +z direction from behind the slot antenna. The electric field vector of the plane wave is in the x direction which is parallel to the width of the slot. The simulation assumes the slots are in an infinite ground plane but shows it as finite.

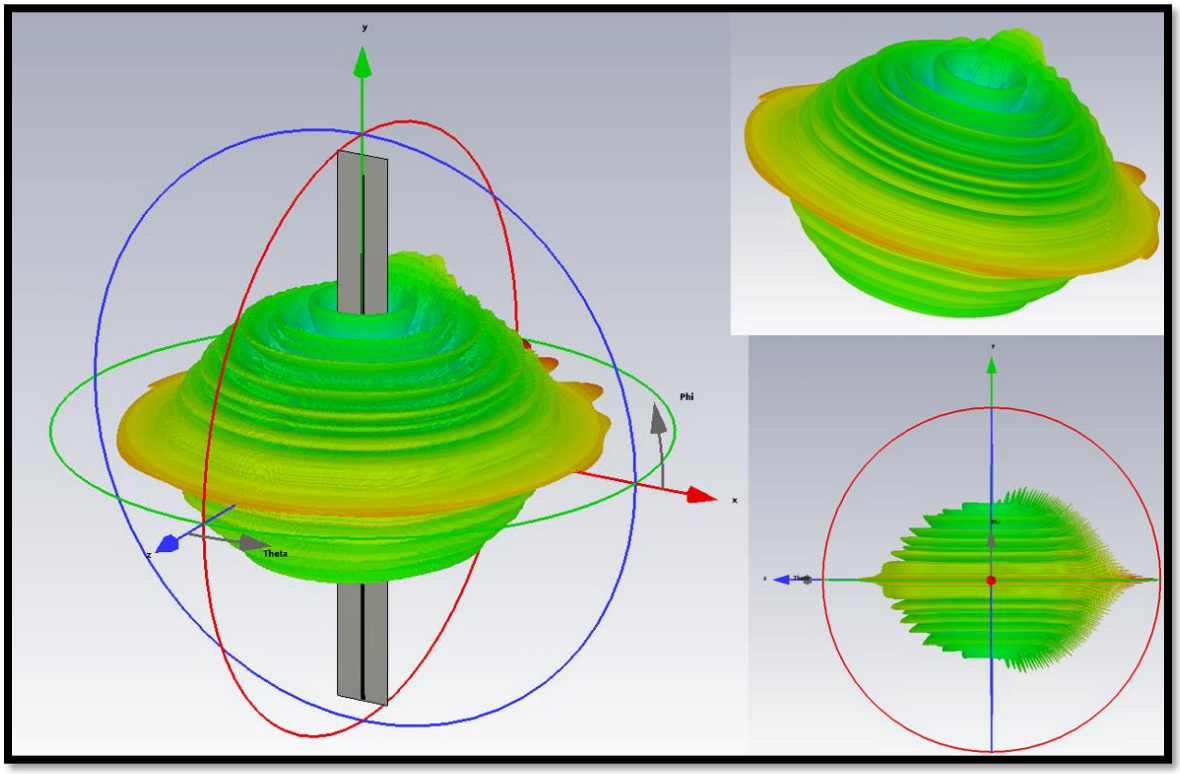

Figure 9 Radiation pattern of the slot array. We are only interested in the wave that passes through the slots that is for $\theta = 0°$ to 90°

brian.scannell@ntlworld.com

The Cartesian pattern cut in Figure 10 shows the antenna pattern nulls versus $\theta°$ for $\phi = 90°$.

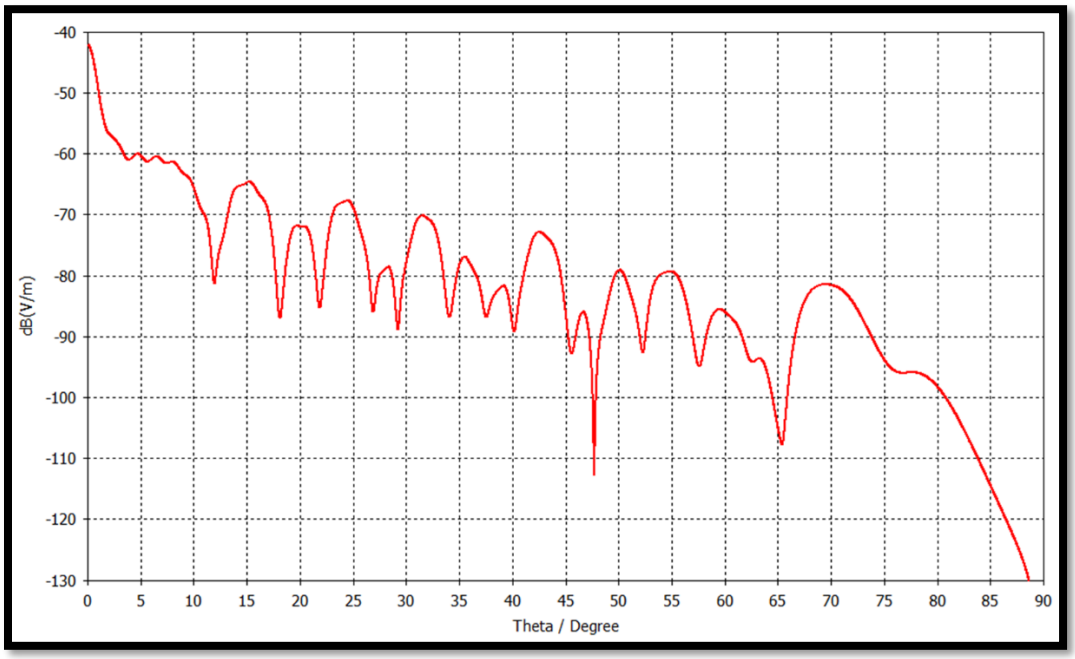

Figure 10 Theta cut of the antenna pattern showing the zero nulls

Table 2 shows the derived zero estimates from the pattern sidelobe nulls.

Zero Number	Sidelobe Null Angle deg	Observed Zero	Zeta Zero	Error %
1	11.93	13.86	14.13	-1.9
2	18.15	20.90	21.02	-0.6
3	21.87	24.99	25.01	-0.1
4	26.94	30.40	30.42	-0.1
5	29.25	32.78	32.94	-0.5
6	34.06	37.57	37.59	0.0
7	37.59	40.93	40.92	0.0
8	40.18	43.28	43.33	-0.1
9	45.57	47.91	48.01	-0.2
10	47.76	49.67	49.77	-0.2
11	52.27	53.06	52.97	0.2
12	57.58	56.63	56.45	0.3
13	62.48	59.50	59.35	0.3
14	65.29	60.95	60.83	0.2

Table 2 Zeros visible from the 500mm slot antenna radiation pattern. Blue entries are not clear nulls

brian.scannell@ntlworld.com

Longer slot array

The longest single antenna that can be manufactured by PCB technology is about 500mm which is the previous design. However, to see larger height nulls it could be possible to arrange three boards lengthwise on a supporting low relative dielectric board (e.g., Rohacell HF31 ε=1.09). This 1500mm antenna is the largest that could be tested in a plane-wave facility called a compact antenna test range (CATR).

This design is shown in Figure 11 and has 1601 slots separated by 0.8mm in y and with a maximum visible zero height of 208 which are the first 85 zeros.

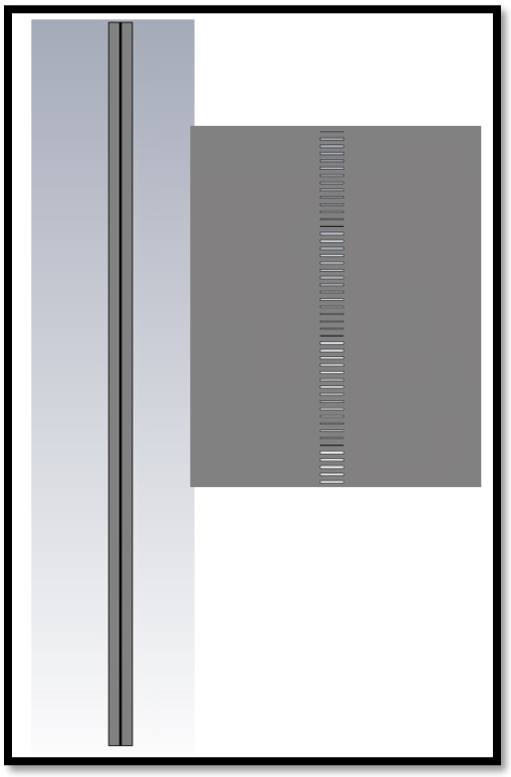

Figure 11 A longer 1500mm slot array

Figures 12 to 14 show various views of the computed radiation patterns.

brian.scannell@ntlworld.com

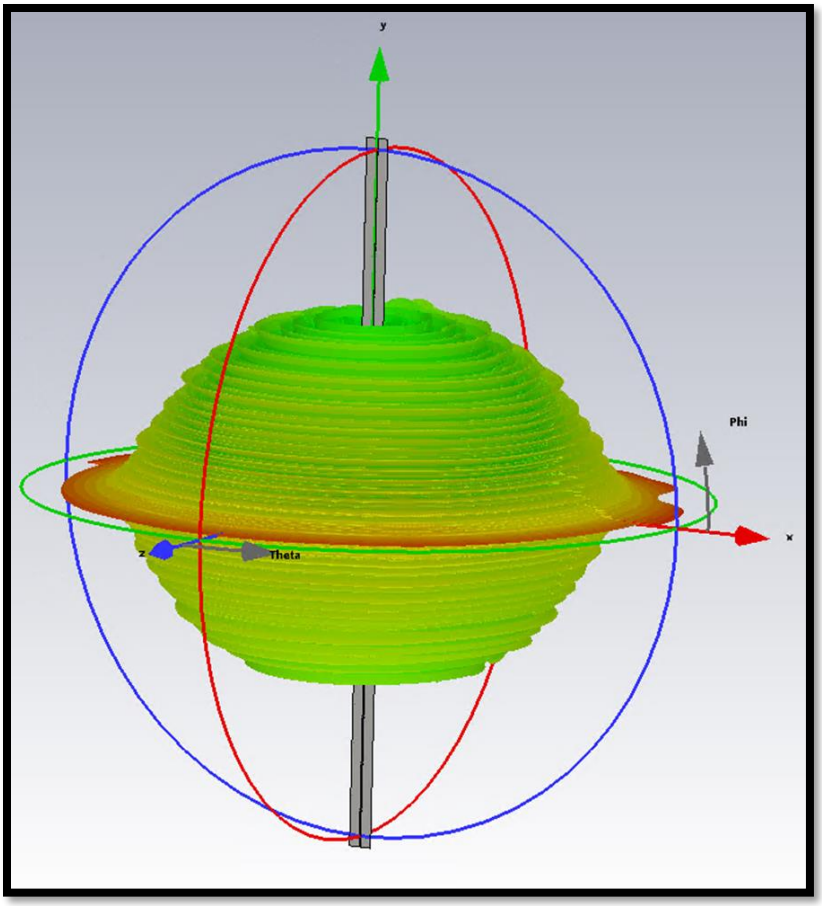

Figure 12 Radiation pattern of the longer slot array

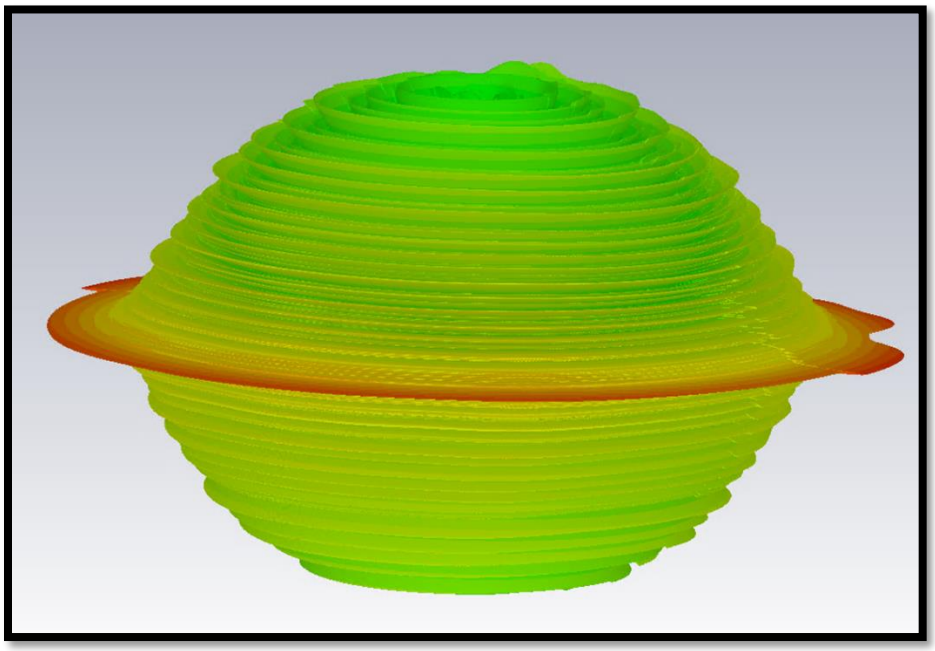

Figure 13 Radiation pattern of the longer slot array

brian.scannell@ntlworld.com

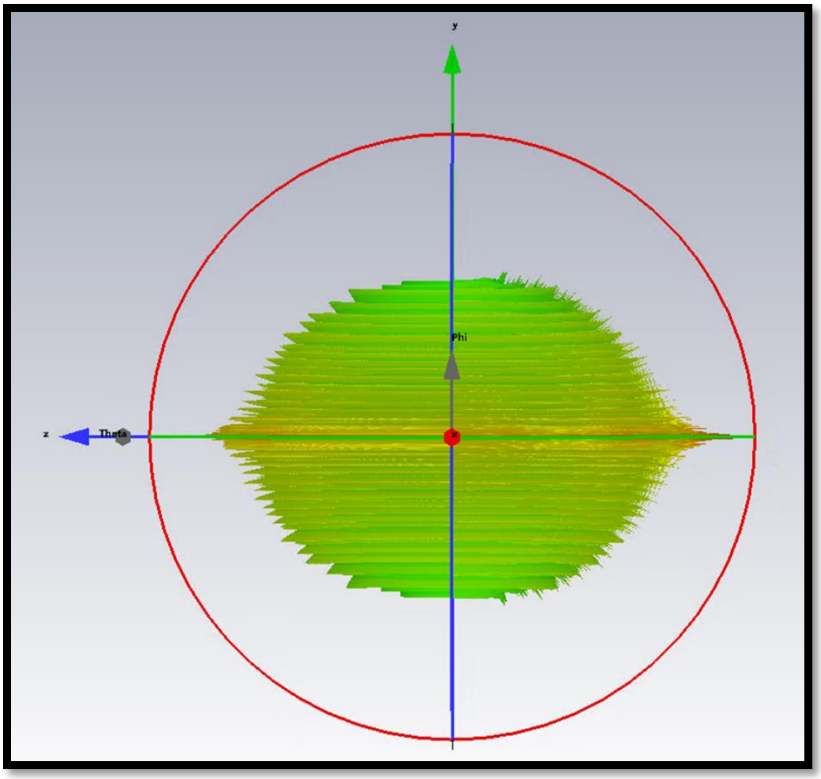

Figure 14 Radiation pattern of the longer slot array

The Cartesian pattern cut in Figure 15 for $\phi = 90°$ shows the larger number of nulls.

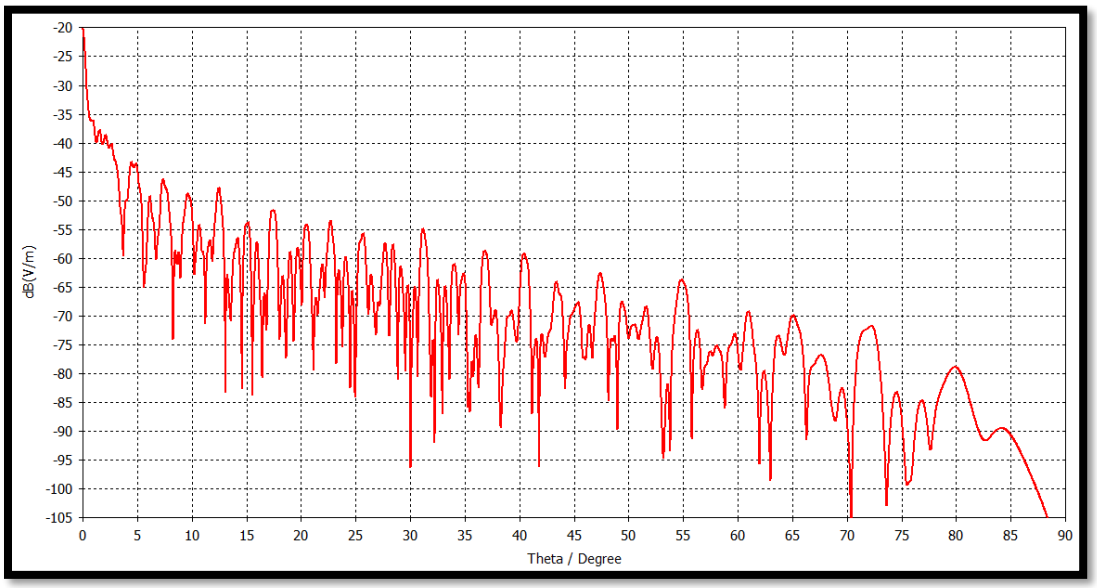

Figure 15 Theta cut of the longer slot array antenna pattern showing more zero nulls

Table 3 shows the 84 derived zero estimates.

brian.scannell@ntlworld.com
August 2021

Zero Number	Sidelobe Null Angle deg	Observed Zero	Zeta Zero	Error %	Zero number	Sidelobe Null Angle deg	Observed Zero	Zeta Zero	Error %
1	3.71	13.58	14.13	-3.9	43	38.29	129.90	129.58	0.2
2	5.71	20.87	21.02	-0.7	44	Not visible		131.09	
3	6.71	24.51	25.01	-2.0	45	39.71	133.96	133.50	0.3
4	8.29	30.21	30.42	-0.7	46	Not visible		134.76	
5	9.00	32.80	32.94	-0.4	47	41.41	138.68	138.12	0.4
6	10.29	37.44	37.59	-0.4	48	41.86	139.89	139.74	0.1
7	11.29	41.03	40.92	0.3	49	42.29	141.06	141.12	0.0
8	11.86	43.08	43.33	-0.6	50	Not visible		143.11	
9	13.14	47.66	48.01	-0.7	51	44.41	146.72	146.00	0.5
10	13.57	49.19	49.77	-1.2	52	Not visible		147.42	
11	14.57	52.74	52.97	-0.4	53	Not visible		150.05	
12	15.57	56.28	56.45	-0.3	54	46.00	150.81	150.93	-0.1
13	16.43	59.29	59.35	-0.1	55	46.71	152.61	153.02	-0.3
14	16.86	60.79	60.83	-0.1	56	48.14	156.15	156.11	0.0
15	18.00	64.79	65.11	-0.5	57	49.00	158.22	157.60	0.4
16	18.57	66.77	67.08	-0.5	58	50.00	160.60	158.85	1.1
17	19.29	69.24	69.55	-0.4	59	Not visible		161.19	
18	20.00	71.70	72.07	-0.5	60	50.86	162.60	163.03	-0.3
19	21.14	75.62	75.70	-0.1	61	52.14	165.53	165.54	0.0
20	21.57	77.08	77.14	-0.1	62	53.14	167.75	167.18	0.3
21	22.14	79.02	79.34	-0.4	63	53.86	169.30	169.09	0.1
22	23.29	82.88	82.91	0.0	64	Not visible		169.91	
23	23.71	84.31	84.74	-0.5	65	55.86	173.51	173.41	0.1
24	24.57	87.18	87.43	-0.3	66	56.76	175.35	174.75	0.3
25	25.00	88.60	88.81	-0.2	67	57.72	177.25	176.44	0.5
26	26.14	92.37	92.49	-0.1	68	Not visible		178.38	
27	26.86	94.71	94.65	0.1	69	58.82	179.36	179.92	-0.3
28	27.18	95.77	95.87	-0.1	70	60.29	182.08	182.21	-0.1
29	28.14	98.89	98.83	0.1	71	62.00	185.11	184.87	0.1
30	28.86	101.18	101.32	-0.1	72	61.98	185.07	185.60	-0.3
31	29.57	103.46	103.73	-0.3	73	62.98	186.77	187.23	-0.2
32	30.00	104.82	105.45	-0.6	74	64.22	188.78	189.42	-0.3
33	30.74	107.16	107.17	0.0	75	66.29	191.95	192.03	0.0
34	31.86	110.65	111.03	-0.3	76	Not visible		193.08	
35	32.22	111.78	111.87	-0.1	77	68.92	195.62	195.27	0.2
36	33.00	114.18	114.32	-0.1	78	Not visible		196.88	
37	33.57	115.93	116.23	-0.3	79	70.40	197.50	198.02	-0.3
38	34.43	118.53	118.79	-0.2	80	73.57	201.09	201.26	-0.1
39	35.29	121.11	121.37	-0.2	81	75.57	203.04	202.49	0.3
40	35.80	122.64	122.95	-0.3	82	Not visible		204.19	
41	36.29	124.07	124.26	-0.1	83	77.71	204.85	205.39	-0.3
42	37.43	127.42	127.52	-0.1	84	82.71	207.95	207.91	0.0

Table 3 Zeros visible from the simulated 1500mm slot antenna radiation pattern. Blue entries are either not visible or not clear nulls

Remarks on the practical difficulties of observing the nulls

Although the larger 1500mm slot array could be tested in a CATR, this would require accommodating a method to view the transmitted wave through the antenna slots rather than the current method of viewing the reflected wave as in radar cross-section measurements. Further, the viewing of this transmitted slot pattern has to be in the far-field which is a large distance and not practically realizable. The only alternative is to near-field probe the transmitted electric fields and then mathematically transform them to a far-field pattern. This secondary viewing aspect is not entirely satisfactory but may be a useful stop-gap until an alternative measurement method is sought.

A second difficultly is to stop the transmission of the diffracted plane wave around the slot array plate which would fill-in the nulls. This could be eased by placing the slot array in a larger metal plate to tie-up more with the simulation condition and then edged with radar absorbing material (RAM) to reduce any forward edge-diffraction.

Conclusion

Computer simulated antenna designs produce radiation patterns which show the Riemann zeros. They are seen clearer than expected from the truncated van der Pol function with umax=3. They generally are within 1% of the true values.

There are practical difficulties to overcome in order to measure the patterns of these designs.

Reference

1) van der Pol B 1947 An electro-mechanical investigation of the Riemann zeta function in the critical strip Bull. Am. Math. Soc. 53 976–81

2) Berry M V 2012 Riemann zeros in radiation patterns J. Phys. A: Math. Theor. 45 302001

brian.scannell@ntlworld.com